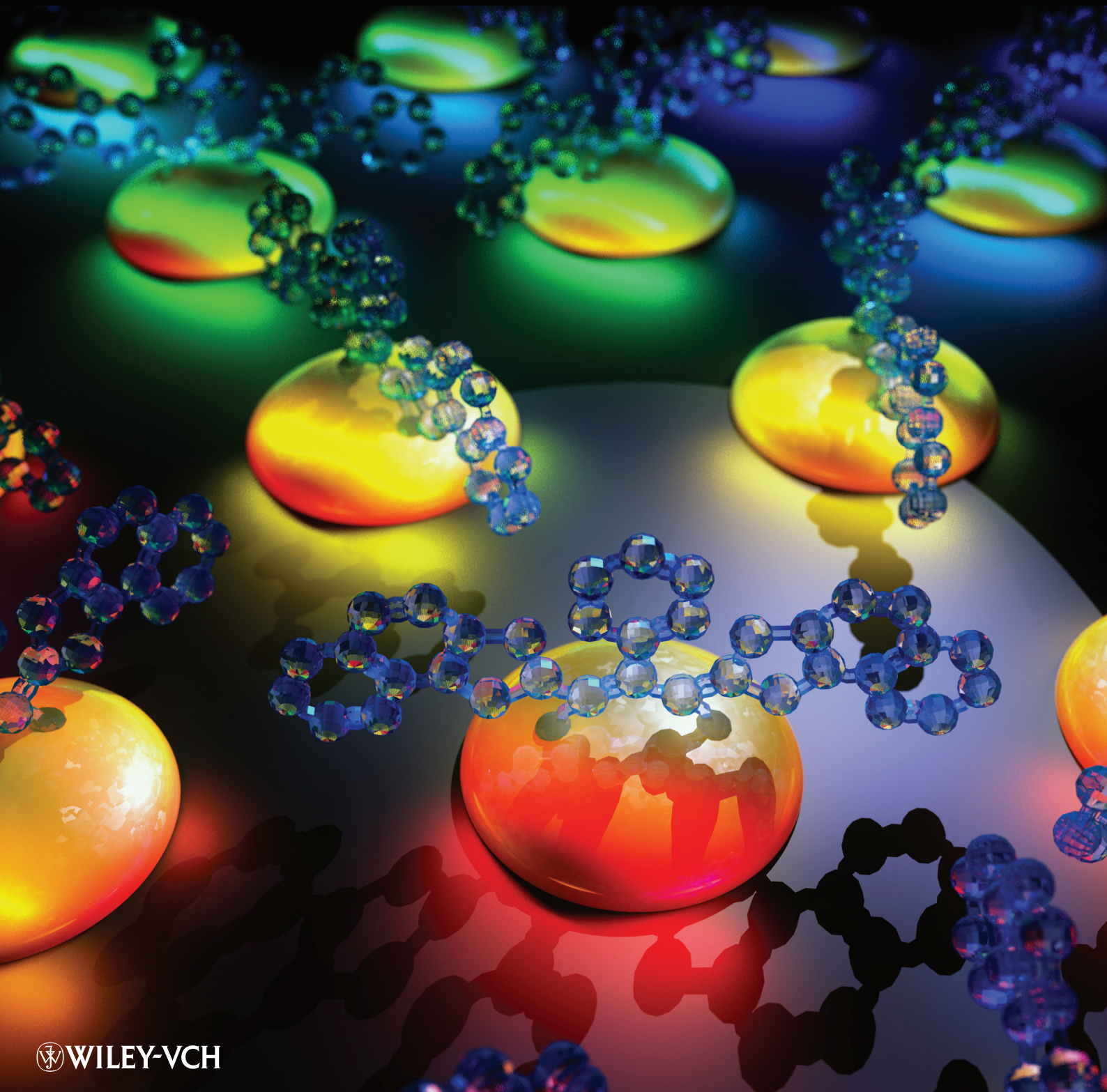


[www.advmat.de](http://www.advmat.de)

# ADVANCED MATERIALS



# Dynamic Tuning of Plasmon–Exciton Coupling in Arrays of Nanodisk–J-aggregate Complexes

By Yue Bing Zheng, Bala Krishna Juluri, Lin Lin Jensen, Daniel Ahmed, Mengqian Lu, Lasse Jensen,\* and Tony Jun Huang\*

Controlling the optical behavior of molecules near the vicinity of noble metal nanoparticles continues to be an active research area in nanoscience and nanotechnology.<sup>[1]</sup> An understanding of the phenomena at such metal-molecule complexes is not only important fundamentally, but also essential for applications such as energy harvesting,<sup>[2]</sup> nanometer-scale optical circuits,<sup>[3]</sup> and ultra-sensitive chemical and biological sensors.<sup>[4]</sup> Of particular interest is the recent discovery of mixed exciton–plasmon states in metal–molecule complexes.<sup>[5–14]</sup> Mixed exciton–plasmon states arise when excitons of molecules, such as J-aggregates,<sup>[15,16]</sup> resonate with the plasmon modes of metal nanoparticles. As a result, new peaks, so-called hybridized states, appear in the extinction spectra; they are governed by the strength of the coupling between excitons and plasmons.<sup>[5,10,11]</sup> The dramatic change in the localized surface plasmon resonance (LSPR) associated with the transition from weak to strong resonant coupling makes the metal-molecule complexes a promising candidate for active molecular plasmonic components such as switches and modulators.<sup>[17]</sup> The combination of these active plasmonic components<sup>[18–25]</sup> with passive components<sup>[26–28]</sup> will enable the development of plasmonic integrated circuits.<sup>[29,30]</sup>

Since resonant coupling strength varies with spectral overlap between LSPR and molecular resonance,<sup>[5,10,11]</sup> a platform with tunable LSPR is essential for understanding and harvesting mixed exciton–plasmon states. In their pioneering work, Wurtz et al. demonstrated tunable exciton–plasmon coupling in J-aggregate-nanorod complexes by varying the thickness of air shells that surround the Au nanorods.<sup>[10]</sup> In another significant work, Fofang et al. used the highly tunable LSPR of Au nanoshells to understand plasmon–exciton coupling as a function of spectral overlap.<sup>[11]</sup> Although these studies demonstrated tunable LSPR by varying plasmon–exciton coupling, they require the fabrication of a large number of different nanoparticles to establish exciton–plasmon hybridization. Such a large number of samples complicate the experimental procedures

and introduce deviations. Furthermore, to change LSPR properties with these methods, one must change the geometry of the nanoparticles, which is not feasible for practical applications such as active nanophotonic devices.

In this Communication, we report the formation of exciton–plasmon states and the in situ dynamic control of the coupling strength in Au nanodisk arrays coated with J-aggregate molecules. By changing the incident angle of incoming light, rather than changing the geometry of the nanoparticles, we observed plasmon–exciton coupling of variable strengths. The experimental data matched well with simulated results based on a coupled dipole approximation (CDA) method. Our approach enabled a simple yet powerful platform for dynamic control of exciton–plasmon coupling—nominal sample sizes are needed to investigate the behavior of resonant coupling and to understand variations in plasmon–exciton coupling strength.

**Figure 1** is the schematic for studying the plasmon–exciton coupling in arrays of nanodisk–J-aggregate complexes. The Au nanodisk arrays were produced on glass substrates using nanosphere lithography (NSL).<sup>[31–33]</sup> The inset in **Figure 1** shows a representative three-dimensional (3D) atomic force microscopy (AFM) image of the Au nanodisk array. The nanodisks have a mean diameter of  $140 \pm 14$  nm, a height of  $20 \pm 2$  nm, and a period of  $320 \pm 32$  nm. For the bare disk array and the J-aggregate-covered disk array, a series of extinction spectra were recorded as the substrate was rotated out-of-plane with an angle  $\theta$ . Further details can be found in the Supporting Information.

To understand the angle-resolved extinction spectra we used CDA<sup>[34,35]</sup> to simulate the extinction spectra of two-dimensional (2D) arrays of Au nanodisks at various incident angles. Details on CDA can be found in the Supporting Information. **Figure 2a** shows a series of angle-resolved extinction spectra from a bare Au nanodisk array. At normal incidence ( $\theta = 0$  degree), a single strong in-plane LSPR was found at a wavelength of 676 nm.<sup>[36]</sup> As the incident angle was changed from 0 to 65 degrees, the peak wavelength continuously redshifted to 710.5 nm. **Figure 2c** shows a series of CDA-simulated extinction spectra for the bare Au spheroid arrays at various incident angles ( $\theta$ ). Each spheroid has a major axis of 110 nm and a minor axis of 17 nm. The simulated results (**Figure 2c**) are in good agreement with the experimental results (**Figure 2a**), showing that the in-plane dipole resonance peak redshifts continuously as  $\theta$  is increased from 0 to 65 degrees.

The spectral angular dependencies arise from the periodicity and the short inter-particle distance of the arrays. The former results in far-field interactions, while the latter near-field interactions (see the Supporting Information for details).<sup>[37–42]</sup> We further find that the angular dependence is dominated by near-field interactions. While the angular dependence of

[\*] Y. B. Zheng, B. K. Juluri, D. Ahmed, M. Lu, Prof. T. J. Huang  
Department of Engineering Science and Mechanics  
The Pennsylvania State University  
University Park, PA 16802 (USA)  
E-mail: junhuang@psu.edu  
Dr. L. L. Jensen, Prof. L. Jensen  
Department of Chemistry  
The Pennsylvania State University  
University Park, PA 16802 (USA)  
E-mail: jensen@chem.psu.edu

DOI: 10.1002/adma.201000251

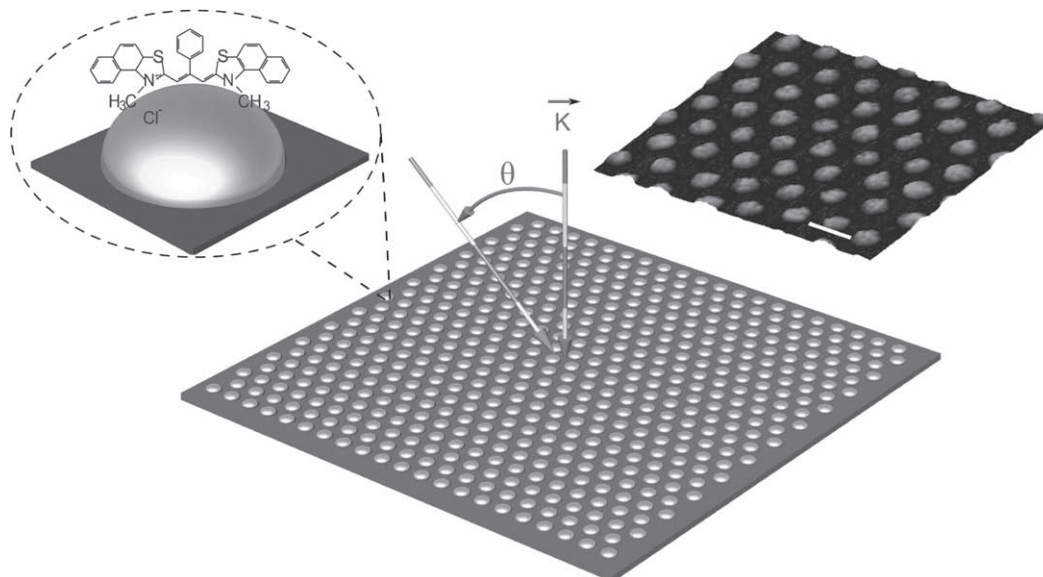


**Figure 1.** A schematic of the arrays of Au nanodisk–J-aggregate complexes and the configuration for angular-resolved spectra. The scale bar in the AFM image is 300 nm.

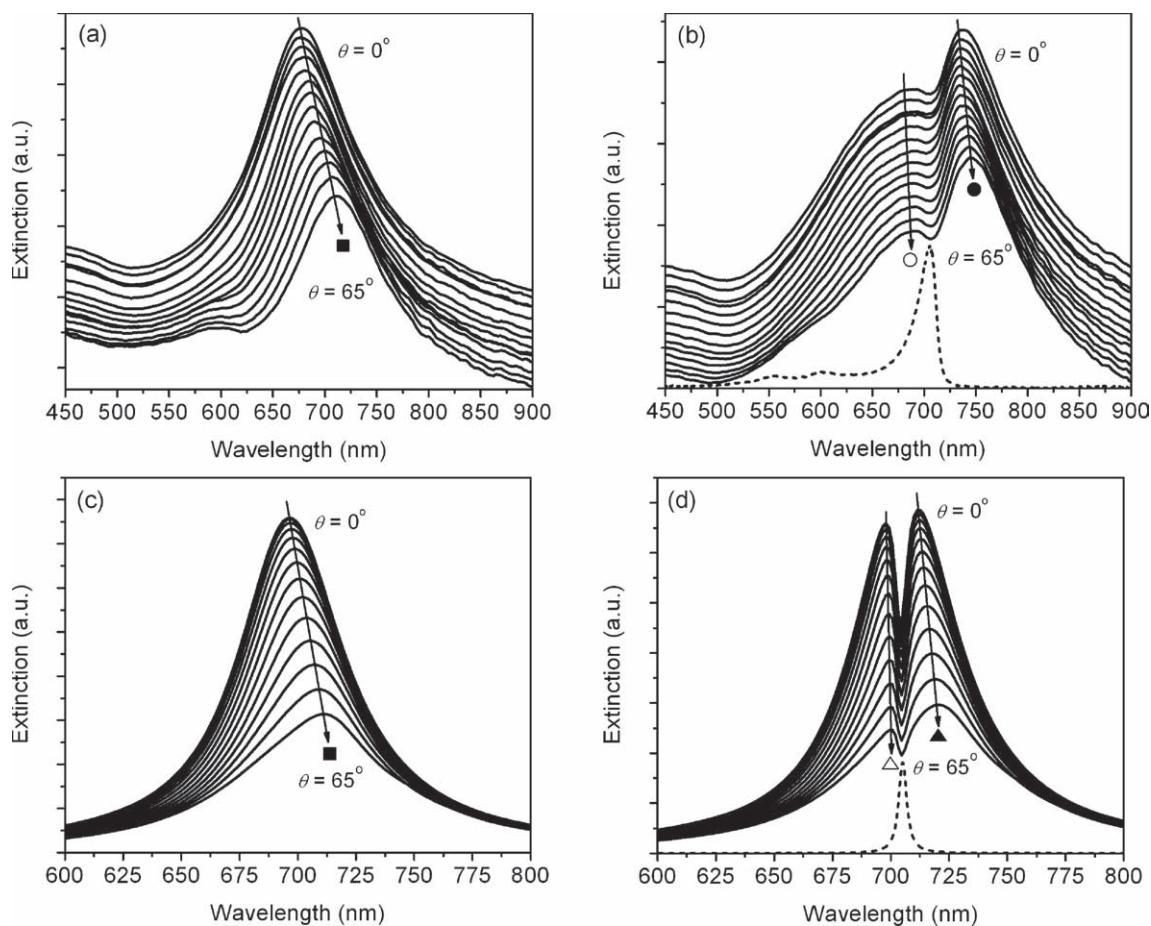


**Figure 2.** a) A series of extinction spectra of the bare Au nanodisk arrays measured at  $\theta$  ranging from 0 to 65 degrees. b) A series of extinction spectra of arrays of nanodisk–J-aggregate complexes measured at  $\theta$  ranging from 0 to 65 degrees. c) A series of simulated extinction spectra of the bare Au spheroid array with incident angle  $\theta$  ranging from 0 to 65 degrees. d) A series of simulated extinction spectra of arrays of Au spheroid–J-aggregate complexes with  $\theta$  ranging from 0 to 65 degrees. The dashed black lines in (b) and (d) are the absorption spectra of J-aggregates without hybridization.

nanoparticle arrays dominated by the far-field interactions is well established,<sup>[35–41]</sup> to our knowledge the details of the effects of near-field coupling on angle dependent spectra have not been reported earlier. It has been shown that the angular dependence for arrays dominated by far-field coupling leads to a non-monotonic shift in the plasmon peak. However, in our case where the interactions are dominated by the near-field coupling, we find monotonic shifts in the plasmon peak with angle, which is better suited for studying the coupling between molecules and nanoparticles. Furthermore, the near field in the nanodisk arrays is relatively insensitive to minor changes in the nanodisk geometries and spacing arising from the NSL.

The angle-resolved extinction spectra for an array of the nanodisk–J-aggregate complexes are shown in Figure 2b. The strong in-plane dipole resonance of the bare Au nanodisk array splits into two bands upon adsorption of J-aggregates on the disk surfaces, reflecting the resonant coupling between plasmons and excitons. The dip between the two extinction peaks corresponds to the absorption peak wavelength of the J-aggregates. Similar to the bare nanodisks, we observe that the two peaks continuously redshift as the incident angle is changed from 0 to 65 degrees. For the nanodisk–J-aggregate complexes, the out-of-plane dipole resonance of the Au nanodisks appears at a wavelength between 550 and 600 nm when the incident angle is increased beyond 40 degrees. For the nanodisk–J-aggregate complexes, the simulated extinction spectra as a function of incident angles (Figure 2d) are also in good agreement with the experimental results (Figure 2b). We see that the in-plane dipole plasmon resonance splits into two hybrid peaks with the dip position corresponding to the absorption peak of the J-aggregates (dashed black line in Figure 2d). Both hybrid peaks redshift as the incident angle  $\theta$  is increased.

In Figure 3a we plot the LSPR peak of the in-plane dipole resonance of the bare nanodisk array (denoted by “Plasmon”) and the two new peaks after the hybridization of the plasmon resonances and molecular excitons (denoted by “Hybrid +” and “Hybrid –” for the high-energy and low-energy peaks, respectively) as a function of the incident angle.<sup>[10]</sup> The hybridization of plasmon resonance and molecular resonance is more obvious in Figure 3b, where we plot the dispersion curves of the “Hybrid +” and “Hybrid –” as a function of “Plasmon”. The bare nanodisk array has a  $\theta$ -tunable range of plasmon energies between 1.745 and 1.833 eV. This energy range is large enough to cover the strong coupling limit due to the hybridization which occurs at 1.76 eV. However, in order to cover a wider energy range, which would reveal both strong and weak coupling between plasmon and exciton resonances, we fabricated a second sample with a  $\theta$ -tunable range of plasmon energies between 1.629 and 1.728 eV. To have the nanodisk arrays of the specific plasmon energies, we tuned NSL parameters combined with the fine-tuning chemical etching process.<sup>[31,33]</sup> We see the characteristic anti-crossing of the two hybrid peaks associated with Rabi splitting of the LSPR peak, where the molecular resonance and the LSPR of the bare nanodisk array overlap. We further notice that the “Hybrid +” curve crosses the solid black line instead of following an asymptotic behavior. This crossing is consistent with Wurtz et al.’s observation on the interaction of plasmon and molecular resonances in the Au nanorod and J-aggregate system.<sup>[10]</sup> The coupling strength is around 125 meV,

consistent with results from nanoshells.<sup>[11]</sup> Thus, by varying the angle of incident light, it is possible to explore the complete energy range necessary for examining the hybridization by using only two samples. Figure 3c shows the simulated LSPR peak energies of the in-plane dipole resonance before and after the hybridization as a function of  $\theta$ . We see that the “Plasmon” peak crosses the “Hybrid +” peak at 25 degrees. In Figure 3d we show the dispersion curves for the nanodisk–J-aggregate complexes. In order to cover the experimental LSPR energy range between 1.629 and 1.833 eV, in the simulation we had to use six different nanoparticles arrays with the same minor axis of 17 nm but different major axes (100, 105, 110, 115, 120, and 125 nm) in the simulations. We see that the simulated dispersion curves (Figure 3d) are in good qualitative agreement with the experimental dispersion curves (Figure 3b)—both simulated and experimental results show peak splitting in the wavelength range where there is spectral overlap between the exciton and the plasmon resonances, and they exhibit the crossing of the “Plasmon” and “Hybrid +” lines at the higher plasmon energies. However, the coupling strength found from the simulations is significantly underestimated as compared to the coupling strength in the experiments. The discrepancy between the experimental and computational results is likely a result of the assumptions made in the CDA model, such as describing the nanodisks as spheroids, using a quasi-static approximation for the polarizability of the spheroids, and describing the substrate as a homogeneous surrounding with an average dielectric constant of glass and air.

Further experiments and simulations reveal that an increased sensitivity of LSPR to the angle of incident light is achievable through the enhanced near-field coupling between the particles by increasing the particle diameter or decreasing the inter-particle spacing (data not shown). However, increasing the near-field coupling also leads to larger redshifts in the LSPR peak, which might not be desirable for some molecules.

In conclusion, we have experimentally and computationally studied the angle-resolved spectra of Au nanodisk arrays with and without J-aggregates. Hybridization of LSPR and exciton resonances has been demonstrated in the nanodisk–J-aggregate using only two samples, one for the weak coupling and the other for the strong coupling. Our method enables efficient measurement of the plasmon–exciton coupling as a function of wavelength, without the need to fabricate new nanoparticle arrays of different LSPR wavelengths. We believe that the angle dependent spectra observed in nanodisk arrays can act as a model system to understand plasmon–exciton interactions. In order to accurately measure the maximum splitting, it is important to maintain the same plasmonic nanostructures, dye morphology, density, and coverage. For example, the plasmon–exciton hybridization is known to increase linearly with the square root of absorbance of the molecular layer.<sup>[43]</sup> However, this level of control and tunability is difficult to achieve in a solid-state platform based on arrays of nanoparticles. Thus, the angle dependent experiments presented in this work opens up the possibility to quantitatively study the interactions between plasmons and excitons with high accuracy.

In cases where measurements in liquid medium are mandatory, recording spectra at variable angles of incidence in liquid flow cells is possible using a variable angle reflection

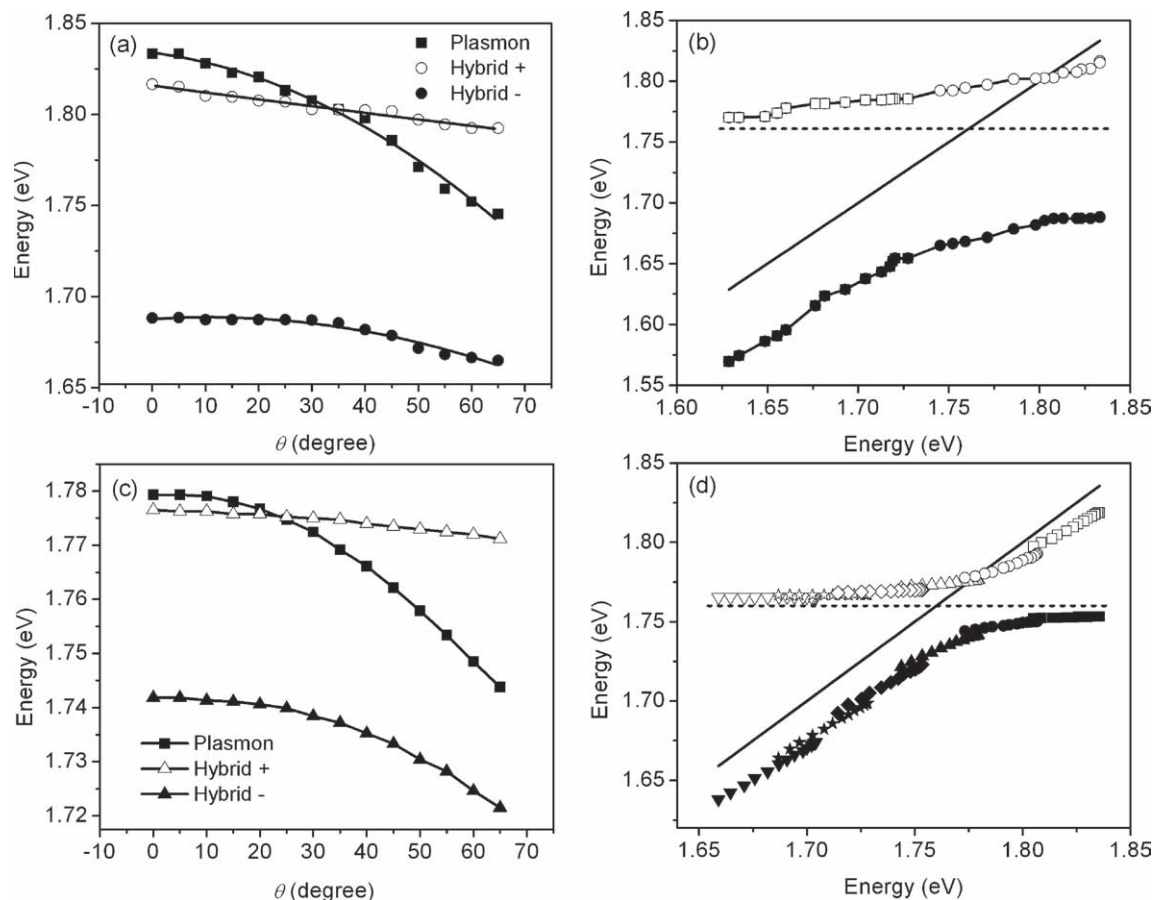


**Figure 3.** a) The peak position of LSPR as a function of  $\theta$  for the nanodisk arrays before and after hybridization. b) The dispersion curves of “Hybrid +” and “Hybrid -” as a function of “Plasmon”. c,d) Theoretical data corresponding to the experimental results in (a,b). Different symbols in (b,d) indicate different samples. The solid and dashed black lines in (b,d) represent the plasmon and exciton energies of nanodisks and J-aggregates before hybridization, respectively.

sampling systems. Our nanodisk arrays can further be integrated into the angular tunable micromirrors used in micro-opto-electro-mechanical systems to realize on-chip tuning of the incident light angle and thus to achieve active control of the exciton–plasmon coupling for applications in plasmonic-optoelectronic devices. With this tunable plasmonic system, one can also study the effects of LSPR on other optical properties of molecules such as fluorescence and Raman spectroscopy, which require precise control of the overlap between the LSPR and the excitation or emission wavelengths. An understanding of these interactions will enable optimization of metal nanoparticle–molecule complexes and have a profound impact on many applications such as active nanophotonic devices,<sup>[3,17,44]</sup> surface-enhanced Raman spectroscopy (SERS),<sup>[45]</sup> and biosensors.<sup>[4]</sup>

Materials, experimental methods, theoretical methods, and origins of angle dependent plasmon spectra can be found in the Supporting Information.

## Supporting Information

Supporting Information is available online from Wiley InterScience or from the author.

## Acknowledgements

Y.B.Z and B.K.J contributed equally to this work. This research was supported by the Air Force Office of Scientific Research (FA9550-08-1-0349), the National Science Foundation (ECCS-0801922, ECCS-0609128, and ECCS-0609128), and the Penn State Center for Nanoscale Science (MRSEC). Components of this work were conducted at the Pennsylvania State University node of the NSF-funded National Nanotechnology Infrastructure Network. Y.B.Z. recognizes the support from KAUST Scholar Award and the Founder’s Prize and Grant of the American Academy of Mechanics. The authors thank I-Kao Chiang, Aitan Lawit and Thomas R. Walker for helpful discussions.

Received: January 21, 2010  
Published online: July 21, 2010

- [1] F. Reil, U. Hohenester, J. R. Krenn, A. Leitner, *Nano Lett.* **2008**, *8*, 4128.
- [2] S. Neretina, W. Qian, E. Dreaden, M. El-Sayed, R. Hughes, J. Preston, P. Mascher, *Nano Lett.* **2009**, *9*, 1242.
- [3] M. L. Brongersma, P. G. Kik, *Surface Plasmon Nanophotonics*, Springer, Berlin, **2007**.
- [4] C. Novo, A. M. Funston, P. Mulvaney, *Nature Nanotech.* **2008**, *3*, 598.
- [5] W. Ni, Z. Yang, H. Chen, L. Li, J. Wang, *J. Am. Chem. Soc.* **2008**, *130*, 6692.

- [6] H. Nishi, T. Asahi, S. Kobatake, *J. Phys. Chem. C* **2009**, *113*, 17359.
- [7] W. A. Murray, W. L. Barnes, *Adv. Mater.* **2007**, *19*, 3771.
- [8] G. Wiederrecht, G. Wurtz, J. Hranisavljevic, *Nano Lett.* **2004**, *4*, 2121.
- [9] Y. Sugawara, T. A. Kelf, J. J. Baumberg, M. E. Abdelsalam, P. N. Bartlett, *Phys. Rev. Lett.* **2006**, *97*, 266808.
- [10] G. Wurtz, P. Evans, W. Hendren, R. Atkinson, W. Dickson, R. Pollard, W. Harrison, C. Bower, A. Zayats, *Nano Lett.* **2007**, *7*, 1297.
- [11] N. T. Fofang, T.-H. Park, O. Neumann, N. A. Mirin, P. Nordlander, N. J. Halas, *Nano Lett.* **2008**, *8*, 3481.
- [12] A. Haes, S. Zou, J. Zhao, G. Schatz, R. VanDuyne, *J. Am. Chem. Soc.* **2006**, *128*, 10905.
- [13] J. Zhao, L. Jensen, J. Sung, S. Zou, G. C. Schatz, R. P. V. Duyne, *J. Am. Chem. Soc.* **2007**, *129*, 7647.
- [14] G. Liu, Y. Long, Y. Choi, T. Kang, L. Lee, *Nat. Methods* **2007**, *4*, 1015.
- [15] *The J-Aggregates*, (Ed: T. Kobayashi) World Scientific, Singapore, **1996**.
- [16] H. van Amerongen, L. Valkunas, R. van Grondelle, *Photosynthetic Excitons*, World Scientific, Singapore, **2000**.
- [17] Y. B. Zheng, Y.-W. Yang, L. Jensen, L. Fang, B. K. Juluri, A. H. Flood, P. S. Weiss, J. F. Stoddart, T. J. Huang, *Nano Lett.* **2009**, *9*, 819.
- [18] P. Andrew, W. L. Barnes, *Science* **2004**, *306*, 1002.
- [19] K. MacDonald, Z. Sámson, M. Stockman, N. Zheludev, *Nature Photonics* **2008**, *3*, 55.
- [20] D. Pacifici, H. Lezec, H. Atwater, *Nature Photonics* **2007**, *1*, 402.
- [21] D. Chang, A. Sørensen, E. Demler, M. Lukin, *Nature Phys.* **2007**, *3*, 807.
- [22] V. K. S. Hsiao, Y. B. Zheng, B. K. Juluri, T. J. Huang, *Adv. Mater.* **2008**, *20*, 3528.
- [23] Y. Leroux, J. C. Lacroix, C. Fave, V. Stockhausen, N. Felidj, J. Grand, A. Hohenau, J. R. Krenn, *Nano Lett.* **2009**, *9*, 2144.
- [24] J. Lee, P. Hernandez, J. Lee, A. Govorov, N. Kotov, *Nat. Mater.* **2007**, *6*, 291.
- [25] G. Wiederrecht, G. Wurtz, A. Bouhelier, *Chem. Phys. Lett.* **2008**, *461*, 171.
- [26] S. I. Bozhevolnyi, V. S. Volkov, E. Devaux, J.-Y. Laluet, T. W. Ebbesen, *Nature* **2006**, *440*, 508.
- [27] S. A. Maier, S. R. Andrews, L. Martín-Moreno, F. J. García-Vidal, *Phys. Rev. Lett.* **2006**, *97*, 176805.
- [28] N. Fang, H. Lee, C. Sun, X. Zhang, *Science* **2005**, *308*, 534.
- [29] H. A. Atwater, S. Maier, A. Polman, J. A. Dionne, L. Sweatlock, *MRS Bull.* **2005**, *30*, 385.
- [30] N. Engheta, *Science* **2007**, *317*, 1698.
- [31] Y. B. Zheng, B. K. Juluri, X. Mao, T. R. Walker, T. J. Huang, *J. Appl. Phys.* **2008**, *103*, 014308.
- [32] Y. B. Zheng, T. J. Huang, A. Y. Desai, S. J. Wang, L. K. Tan, H. Gao, A. C. H. Huan, *Appl. Phys. Lett.* **2007**, *90*, 183117.
- [33] Y. B. Zheng, L. Jensen, W. Yan, T. R. Walker, B. K. Juluri, L. Jensen, T. J. Huang, *J. Phys. Chem. C* **2009**, *113*, 7019.
- [34] E. M. Purcell, C. R. Pennypacker, *Astrophys. J.* **1973**, *186*, 705.
- [35] L. Zhao, K. L. Kelly, G. C. Schatz, *J. Phys. Chem. B* **2003**, *107*, 7343.
- [36] K. B. Crozier, E. Togan, E. Simsek, T. Yang, *Opt. Express* **2007**, *15*, 17482.
- [37] N. Féridj, G. Laurent, J. Aubard, G. Lévi, A. Hohenau, J. Krenn, F. Aussenegg, *J. Chem. Phys.* **2005**, *123*, 221103.
- [38] M. Meier, A. Wokaun, P. Liao, *J. Opt. Soc. Am. B*, **1985**, *2*, 931.
- [39] B. Lamprecht, G. Schider, R. Lechner, H. Ditlbacher, J. Krenn, A. Leitner, F. Aussenegg, *Phys. Rev. Lett.* **2000**, *84*, 4721.
- [40] Y. Chu, E. Schonbrun, T. Yang, K. Crozier, *Appl. Phys. Lett.* **2008**, *93*, 181108.
- [41] A. O. Pinchuk, *J. Phys. Chem. A* **2009**, *113*, 4430.
- [42] A. Bouhelier, R. Bachelot, J. S. Im, G. P. Wiederrecht, G. Lerondel, S. Kostcheev, P. Royer, *J. Phys. Chem. B* **2005**, *109*, 3195.
- [43] B. K. Juluri, M. Lu, Y. B. Zheng, L. Jensen, T. J. Huang, *J. Phys. Chem. C* **2009**, *113*, 18499.
- [44] B. K. Juluri, Y. B. Zheng, D. Ahmed, L. Jensen, T. J. Huang, *J. Phys. Chem. C* **2008**, *112*, 7309.
- [45] G. C. Schatz, R. P. Van Duyne, *Electromagnetic Mechanism of Surface-Enhanced Spectroscopy*, Wiley, Chichester, UK **2002**.